Croatian Society for Materials Protection

Metalurgija/Metallurgy

Vol. 66 No. 2 / 2027

Simulation of Air-Jet Cooling of a Moving Steel Block during On-Line Heat Treatment

L. X. Y. Xiao [1], Y. Wang [2], L. C. Xu [2], Z. B. Li [2], W. L. Huo [1], and M. X. Gao [2,*]

https://doi.org/10.64486/m.66.2.4

[1] School of Material and Metallurgy, University of Science and Technology Liaoning, Anshan, China
[2] School of Innovation and Entrepreneurship, University of Science and Technology Liaoning, Anshan, China
* Correspondence: e-mail: gaoming31@163.com

Type of the Paper: Article
Received: April 8, 2026
Accepted: August 3, 2026

Abstract: Precise control of jet cooling rate is critical to optimizing the on-line heat treatment process for steel rails. Numerical simulation can effectively shorten the research cycle and reduce costs. Most existing simulations of jet cooling for high-temperature steel are based on static nozzles and stationary rails, which deviate from the continuous movement of rails in actual production and compromise simulation accuracy. To improve the consistency between simulation and real working conditions, this study adopts sliding mesh and overset mesh techniques to numerically simulate jet cooling of a moving high-temperature steel block. Reciprocating experiments are conducted to compare simulation results under three conditions—static, moving with sliding mesh, and moving with overset mesh—with experimental data. Results show that the average relative errors compared with experiments are 18.01 %, 14.88 %, and 13.36 %, respectively, and the relative deviations of cooling uniformity standard deviation against experimental data are 92.59 %, 7.41 %, and 22.22 %, respectively. In conclusion, the overset mesh model yields higher accuracy in overall temperature field prediction, while the sliding mesh model achieves better agreement with experimental results in terms of cooling uniformity. Both dynamic mesh methods improve consistency with actual working conditions compared with the stationary model.

Keywords: moving steel block; air-jet impingement cooling; overset mesh; sliding mesh; transient heat transfer; cooling uniformity

1. Introduction

Air-jet cooling technology utilizes nozzles to impinge compressed air onto the surface of high-temperature workpieces, thereby achieving controllable accelerated cooling. Owing to its advantages of adjustable cooling rates and stable post-cooling microstructure and properties, this technique has become the primary cooling method in the on-line heat treatment of rails. The selection of air-jet process parameters directly determines the final material quality and production efficiency after cooling. Therefore, a clear understanding of the heat transfer characteristics during air-jet cooling is a prerequisite for process parameter design.

Due to its advantages of low cost and short development cycle, numerical simulation has been widely applied in the field of controlled cooling of steel after rolling [1–3]. As shown in Figure 1, in actual production, rails in the austenitic state after rolling are directly transferred into the heat treatment unit for air-jet cooling. During the entire cooling process, the rails remain in continuous motion. Evidently, simulations based on a stationary assumption deviate from real moving conditions, which affects the accuracy of the results. Therefore, it is necessary to carry out simulation studies on air-jet cooling in on-line heat treatment under moving conditions. However, most existing studies are still based on the assumption of relative stationarity between the rail and the nozzles [4–7].

With regard to numerical simulation of moving fields, extensive applications have been reported in fields such as shipbuilding and automotive engineering. The key lies in the selection of dynamic mesh techniques, including overset mesh, sliding mesh, deforming mesh with local remeshing, and Cartesian grid methods [8,9]. Among these, overset mesh and sliding mesh are more suitable for simulating the relative translational motion of rigid bodies [10,11].

In terms of overset mesh applications, Xu Jiaqi et al. [12] compared its performance in propeller hydrodynamic simulations and found that the predicted thrust coefficients were closer to experimental values. Zhang Dapeng et al. [13] applied it to the simulation of fully appended submarine maneuvering motion and pointed out that there is still room for improvement in balancing computational accuracy and efficiency. Chen Mo et al. [14] verified the effectiveness of the overset mesh method in simulations of propeller cavitation and submarine self-propulsion.

Regarding sliding mesh applications, Zhou Huifeng [15] proposed a hybrid mesh technique with nested multiple sliding meshes to investigate the hydrodynamic characteristics of underwater robots. Zhao Fan et al. [16] employed the sliding mesh method to analyze vehicle speed control strategies during train passing scenarios. Bojanowski C et al. [17] adopted the sliding mesh approach to carry out unsteady RANS CFD simulations for aerodynamic gust loads induced by moving trucks, which provides a mature reference for simulating rigid-body translational relative motion in transient flow fields.

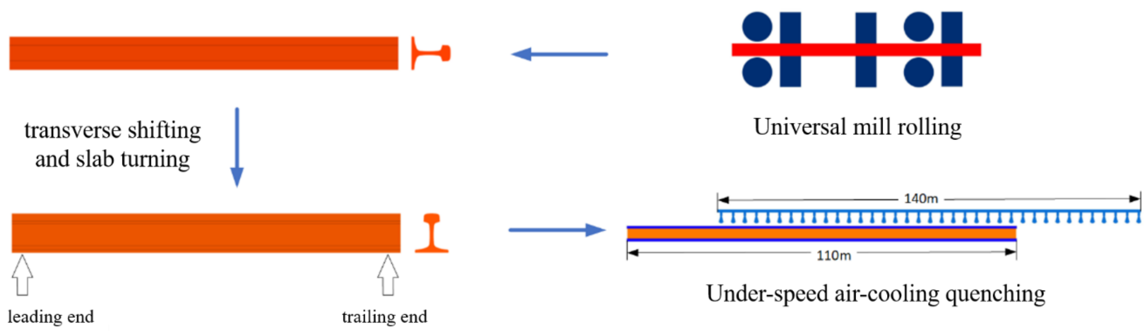

Figure 1. Schematic diagram of the on-line heat treatment production process for rails

Although overset and sliding mesh methods have been widely applied in hydrodynamic and aerodynamic moving-boundary simulations, to the authors' knowledge, few published studies have investigated transient heat-transfer simulations of jet-impingement cooling for continuously moving high-temperature steel workpieces. Most existing rail-cooling simulations are based on a stationary-workpiece assumption, which does not account for the continuous translational motion occurring in actual production and may affect temperature-prediction accuracy. Such moving-boundary coupled simulations involve significant challenges, as they must simultaneously address large temperature gradients (from room temperature to 900 °C), high velocity gradients (jet velocities ranging from 0 m/s to 340 m/s), and the strong coupling associated with moving fluid-solid boundaries.

In this study, taking the on-line heat treatment process of rails as the engineering background, numerical simulations of air-jet cooling for a moving steel block were carried out using both the overset mesh and sliding mesh methods. An in-house experimental platform was established for validation, and a comprehensive comparison was conducted to evaluate the advantages and limitations of the two mesh techniques in terms of computational accuracy.

 https://doi.org/10.64486/m.66.2.4

2. Simulation Model

2.1. Geometric Model

U75V rail steel was selected as the research material, with a Poisson's ratio of 0.3 and a density of 7860 kg/m^3. The temperature-dependent thermophysical properties are listed in Table 1 [6]. The primary objective of this study is to compare the influence of different mesh techniques on computational accuracy. To simplify the model and reduce computational cost, the rail head geometry was approximated as a rectangular steel block with dimensions of 60 mm × 50 mm × 35 mm.

Table 1. Thermophysical properties of U75V steel [6]

Temperature °C	**Specific Heat Capacity** J·(kg·°C)$^{-1}$	**Thermal Conductivity** W·(m·°C)$^{-1}$	**Enthalpy** J·m^{-3}
100	480	37	3.82 × 10^8
200	500	35	7.72 × 10^8
300	510	33	11.7 × 10^8
400	550	31	15.97 × 10^8
500	620	30	20.78 × 10^8
600	680	28	25.95 × 10^8
700	700	23	37.54 × 10^8
800	500	19	41.81 × 10^8
900	570	23	49.14 × 10^8
1000	580	25	53.85 × 10^8

A conventional converging nozzle, as used in industrial production, was employed for the cooling process. Its geometry is illustrated in Figure 2, with an outlet diameter of 7 mm and a total length of 45 mm. The relative arrangement between the nozzles and the steel block is shown in Figure 3. A total of five nozzles were installed with a spacing of 30 mm, and the distance between the nozzle outlets and the upper surface of the steel block was set to 60 mm.

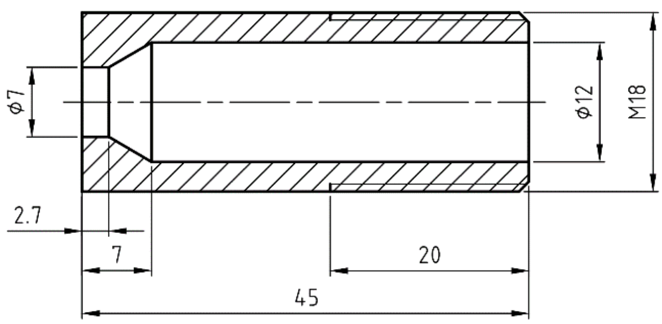

Figure 2. Ordinary converging nozzle

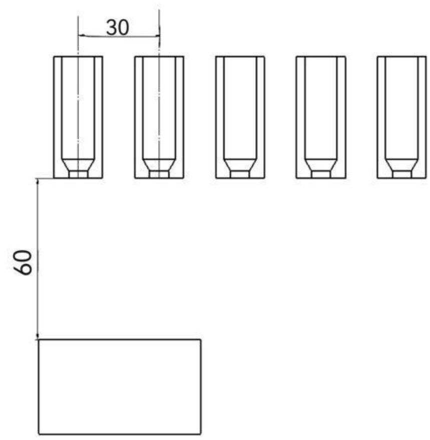

Figure 3. Relative position of nozzles and steel block

https://doi.org/10.64486/m.66.2.4

2.2 Meshing

2.2.1 Overset Mesh

The overset mesh consists of two components: a background mesh and a foreground mesh. The background mesh covers the entire computational domain and provides a fixed computational framework, while the foreground mesh encloses the moving object (steel block) and is allowed to move independently relative to the background mesh. The two mesh systems overlap spatially. Prior to computation, preprocessing procedures, including hole-cutting, node selection, and interpolation, are performed to establish data communication between the overlapping grids [18]. In the present study, the background computational domain is defined as 500 mm × 300 mm × 245 mm. The steel block together with the surrounding fluid region is defined as the foreground (overset) mesh, forming the overset interface with the adjacent fluid domain. The foreground mesh completely wraps the steel block and moves synchronously with it, while the background mesh remains fixed as the outer fluid domain. A structured hexahedral mesh is employed throughout, with local refinement applied at the solid–fluid interfaces (steel block and nozzles). A schematic of the overset mesh configuration is shown in Figure 4, with a total mesh count of approximately 3.96 million cells.

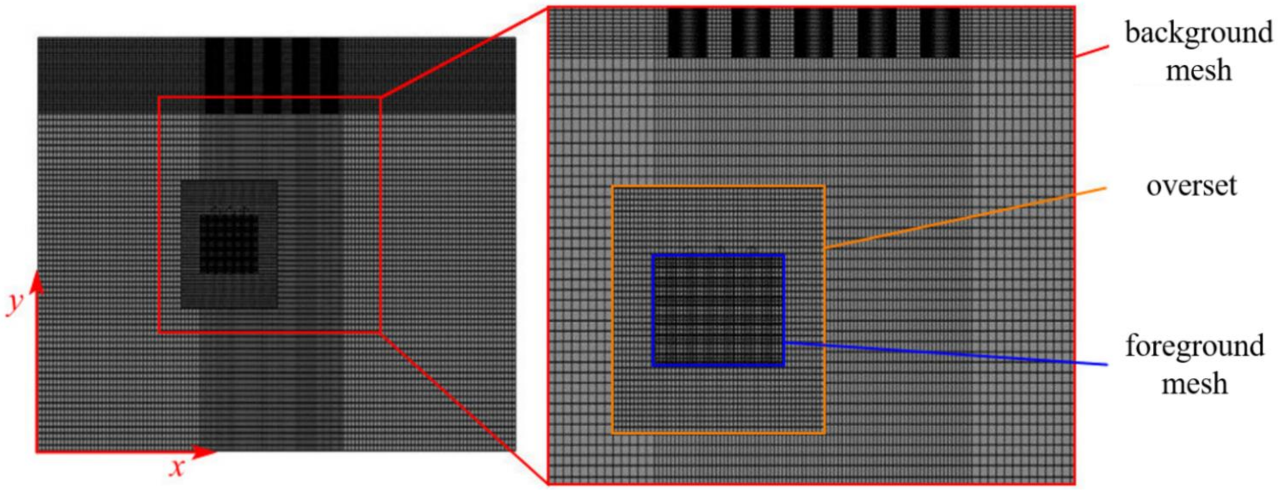

Figure 4. Overset mesh computational domain

2.2.2 Sliding Mesh

In the sliding mesh approach, the computational domain is divided into an upper stationary region (containing the nozzles) and a lower moving region (containing the steel block). The two regions are meshed independently, and a sliding interface is defined at their junction. During the motion of the moving domain, flux continuity across the interface is ensured through interpolation between adjacent mesh cells. In the present study, the stationary domain has dimensions of 500 mm × 300 mm × 75 mm, while the moving domain measures 360 mm × 300 mm × 155 mm. The mesh size ratio across the sliding interface is set to 2:1. Similarly, local mesh refinement is applied at the solid–fluid interfaces. A schematic of the sliding mesh configuration is shown in Figure 5, and the total number of mesh cells is approximately 2.78 million.

https://doi.org/10.64486/m.66.2.4

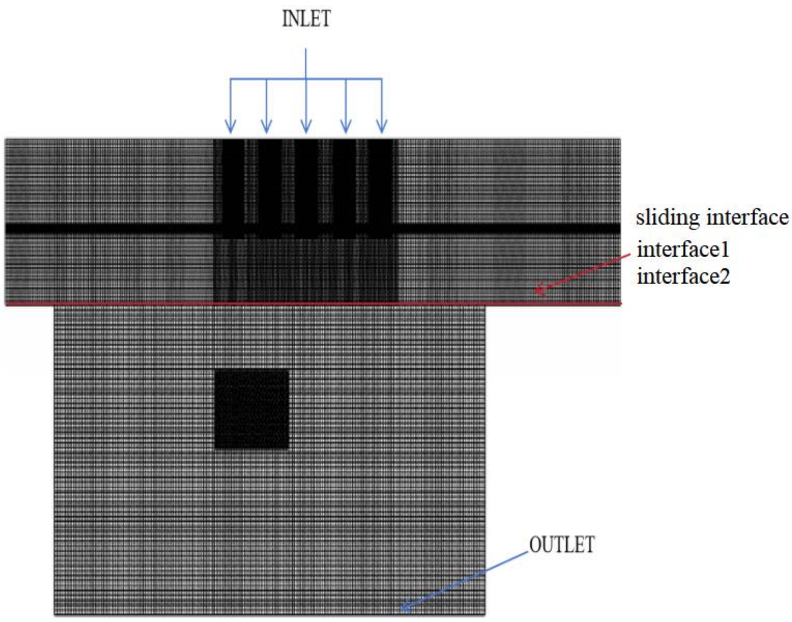

Figure 5. Sliding mesh model meshing

2.3 Boundary Conditions and Initial Conditions

The nozzle inlet was defined as a pressure inlet with a pressure of 0.2 MPa and a temperature of 26.85 °C. The lower boundary of the fluid domain was specified as a pressure outlet with a pressure of 0 Pa. All walls were assigned no-slip and adiabatic boundary conditions. Among them, the nozzle walls were treated as stationary no-slip walls, while the surface of the steel block was defined as a moving no-slip wall. The initial temperature of the steel block was set to 900 °C, while the initial temperature of the fluid domain was 26.85 °C. Gravitational acceleration was applied in the negative Y-direction with a magnitude of 9.81 m/s^2. The cooling medium was assumed to be ideal air, and the wall roughness was set to 0.5 μm. The steel block reciprocated along the X-direction beneath the nozzles at a velocity of 0.04 m/s. The stroke corresponded to the nozzle coverage region, with one complete reciprocating cycle every 5 s, and a total cooling duration of 35 s.

2.4 Numerical Method

The numerical simulations were carried out using the Fluent solver based on the finite volume method. The Realizable k–ε turbulence model was selected for this study. Compared with the standard k–ε model, the Realizable k–ε model improves the calculation accuracy of rotational flow, boundary layer flow and jet impingement flow by introducing a revised turbulent viscosity formula and a transport equation for the dissipation rate. For the present air-jet impingement cooling scenario with high velocity gradient and strong wall shear, the Realizable k–ε model can more accurately capture the flow structure in the impingement zone and the development of the thermal boundary layer, and has been widely verified and applied in similar air-jet impingement cooling studies of high-temperature steel [6, 19]. The SST k–ω model was also considered in the pre-research stage, but it requires higher mesh resolution near the wall and larger computational cost for the current dynamic mesh system, while the prediction accuracy of the overall temperature field is not significantly different from that of the Realizable k–ε model. Therefore, the Realizable k–ε model was finally selected to balance computational accuracy and efficiency [20]. The turbulent Prandtl numbers for turbulent kinetic energy and dissipation rate were set to 1.0 and 1.3, respectively. Both the convective and diffusive terms were

 https://doi.org/10.64486/m.66.2.4

discretized using a second-order upwind scheme, and the pressure–velocity coupling was handled using the Coupled algorithm. The under-relaxation factor was set to 0.75. During the computation, a steady-state solution was first obtained to establish a stable flow field. Subsequently, the solver was switched to a transient formulation, in which the motion of the steel block was activated and the temperature field was solved.

2.5 Mesh and Time Step Independence Verification

To ensure the reliability of the simulation results and eliminate the influence of mesh resolution and time step size on calculation accuracy, mesh independence verification and time step independence verification were carried out respectively.

For mesh independence verification, three sets of meshes with different resolutions were designed for both the overset mesh model and the sliding mesh model, with the central point temperature of the steel block after 35 s of cooling as the evaluation index. For the overset mesh model, the total number of cells of the three sets of meshes was 2.12 million, 3.96 million and 6.08 million respectively. The calculated central point temperatures were 523.7 °C, 512.4 °C and 509.8 °C respectively. The relative deviation between the 3.96 million mesh and the 6.08 million mesh was 0.51 %, which was less than 1 %, indicating that the calculation accuracy was no longer significantly improved with the increase of mesh number. For the sliding mesh model, the total number of cells of the three sets of meshes was 1.54 million, 2.78 million and 4.25 million respectively. The calculated central point temperatures were 531.2 °C, 519.6 °C and 517.1 °C respectively. The relative deviation between the 2.78 million mesh and the 4.25 million mesh was 0.48 %, which also met the independence requirement. Therefore, the 3.96 million overset mesh and 2.78 million sliding mesh were selected for subsequent calculation to balance computational accuracy and efficiency.

For time step independence verification, three time step sizes of 0.01 s, 0.02 s and 0.05 s were selected for comparative calculation under the overset mesh model. The central point temperatures after 35 s of cooling were 511.8 °C, 512.4 °C and 515.7 °C respectively. The relative deviation between the 0.02 s time step and the 0.01 s time step was 0.12 %, which was negligible. Considering the computational efficiency and the requirement of capturing the transient temperature change during the movement of the steel block, 0.02 s was selected as the time step size for all transient simulations in this study.

3. Experimental Validation

To validate the accuracy of the numerical model, an air-jet cooling experimental setup was constructed, as shown in Figure 6. The apparatus mainly consists of five nozzles (1), a support frame (2), a coupling (3), and a reciprocating motor (4). The experimental setup used the same five-nozzle configuration as the numerical model, with identical nozzle spacing, stand-off distance, and inlet pressure. The motor drives the steel block mounted on the platform to perform reciprocating linear motion via a coupling and a lead screw slide table. The motion velocity and reversal timing are controlled by a time relay and a speed controller. Compressed air supplied by an air compressor is delivered to the nozzles after passing through a pressure-stabilizing tank and a pressure regulating valve.

The temperature at designated points on the upper surface of the steel block was measured using an Optris CS laser 2M infrared thermometer (model 6720076). This infrared thermometer has a temperature measurement range of 385 °C–1600 °C, a short spectral response band of approximately 1.6 μm, and a measurement accuracy of ±0.3 % of the measured value plus ±2 °C. Emissivity calibration was performed prior to formal experiments using a comparison method. First, the test specimen was heated to the target temperature in a pre-calibrated heating furnace, with its surface covered by thermal insulation material inside the furnace to reduce heat loss

 https://doi.org/10.64486/m.66.2.4

during transfer. Next, the specimen was taken out of the furnace and immediately placed at the predetermined measurement position. The insulation material was then removed, and the surface temperature was detected by the infrared thermometer, and the emissivity parameter of the instrument was adjusted iteratively until the measured reading was consistent with the preset furnace temperature. The calibrated emissivity value of 0.85 was adopted for all temperature data acquisition in the experiments.

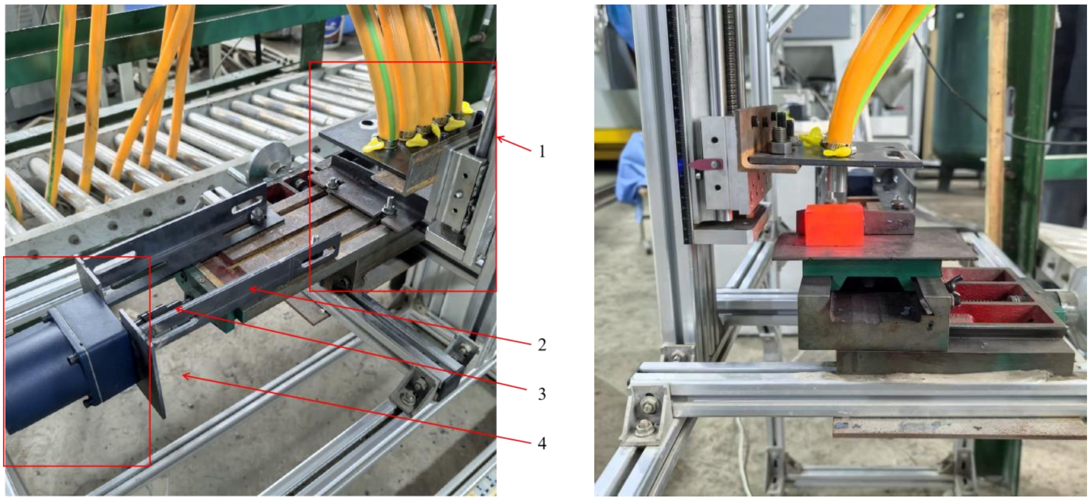

Figure 6. Cooling actuator

4. Results and Analysis

Three temperature monitoring points were defined on the upper surface of the steel block: the central point B, and two additional points A and C located 15 mm on either side of point B along the direction of motion (X-direction). The temperature evolution curves obtained from numerical simulations at these points were compared with the experimental results. The relative error at each monitoring point x (x = A, B, C) is defined as:

$$RU(x) = \left| \frac{\text{experimental value} - \text{calculated value}}{\text{experimental value}} \right| \times 100 \tag{1}$$

Figures 7, 8, and 9 present the comparisons between the simulated and experimental temperature variations at the monitoring points as a function of time under three conditions: the stationary state, the moving state based on the sliding mesh method, and the moving state based on the overset mesh method, corresponding to Figure 7, 8 and 9 respectively. In each figure, the left vertical axis corresponds to the temperature curves of the monitoring points, and the right vertical axis corresponds to the relative error of each point. Specifically, curves A, B and C represent the simulated temperature results at the three monitoring points, while curves a, b and c denote the corresponding experimental measurement results.

https://doi.org/10.64486/m.66.2.4

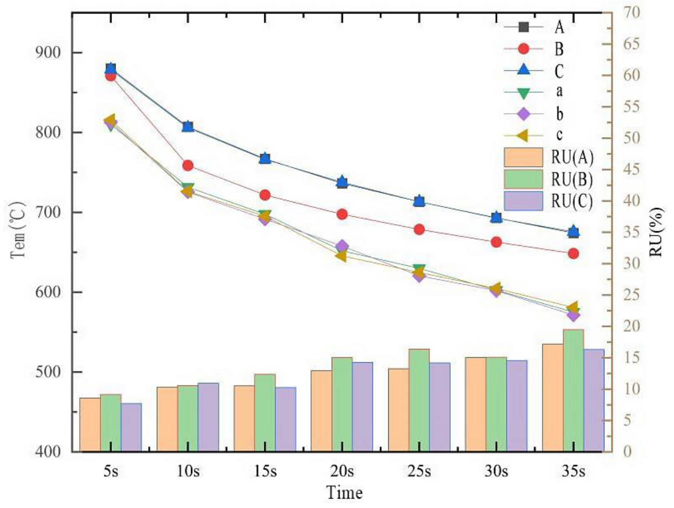

Figure 7. Comparison between stationary simulation and experimental results

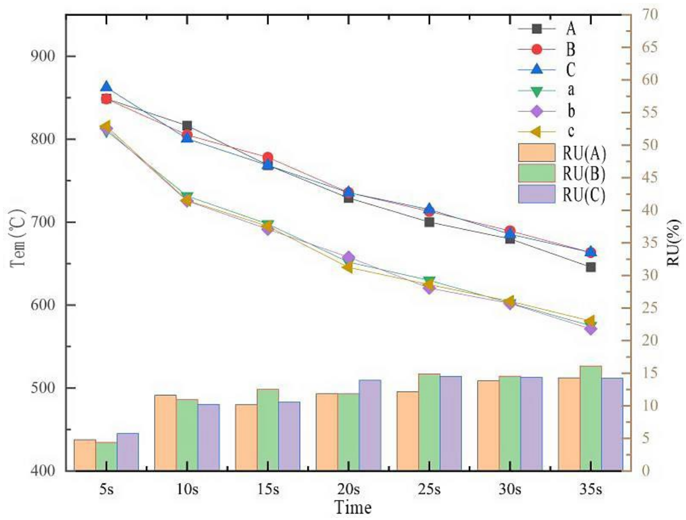

Figure 8. Comparison between sliding mesh moving simulation and experimental results

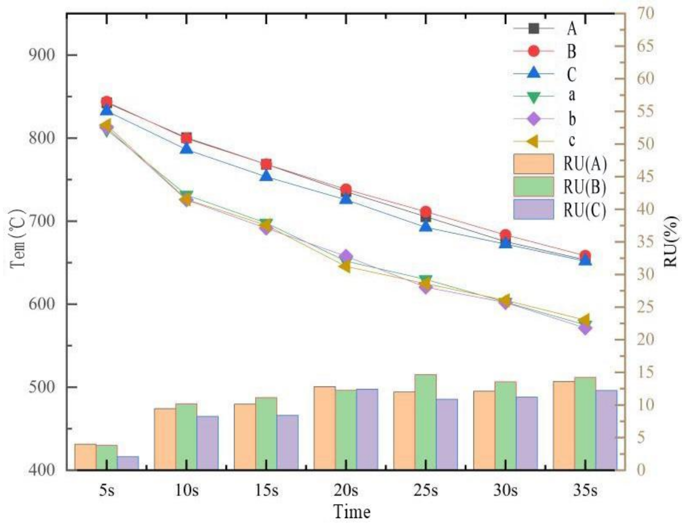

Figure 9. Comparison between overset mesh moving simulation and experimental results

https://doi.org/10.64486/m.66.2.4

After 35 s of cooling, the comparison of errors between the three simulation approaches and the experimental results is summarized in Table 2. For the stationary simulation, the maximum relative errors at the monitoring points are 17.21 %, 19.49 %, and 17.33 %, respectively, with an average relative error of 18.01 %. For the moving simulation based on the sliding mesh method, the average relative error is 14.88 %, while for the overset mesh method, it is further reduced to 13.36 %. Compared with the stationary case, the mean relative error decreases from 18.01 % to 14.88 % for the sliding mesh method and to 13.36 % for the overset mesh method, corresponding to reductions of 3.13 and 4.65 percentage points, respectively. These results indicate that accounting for the motion of the steel block can effectively improve the accuracy of the simulation.

Table 2. Comparison of temperature errors among three simulations and experiment

Simulation type	Maximum relative errors at points A, B, and C / %	Mean relative error / %
Stationary State	17.21, 19.49, 17.33	18.01
Sliding Mesh Motion	14.30, 16.11, 14.24	14.88
Overset Mesh Motion	13.62, 14.23, 12.24	13.36

In industrial production, the cooling rate and its uniformity are critical factors determining the final microstructure and mechanical properties of rails. Since the rail moves at a constant speed, the cooling rate at different points across its cross-section is theoretically expected to be uniform. To quantify the uniformity of cooling rates at three measurement points, the standard deviation (*Dev*) is introduced as an evaluation metric:

$$Dev = \sqrt{\frac{1}{n-1}\sum_{i=1}^{n}(X_i - \bar{X})^2} \tag{2}$$

In the formula, X_i represents the average cooling rate at measurement point i during the cooling period, and $\bar{X}$ denotes the mean cooling rate across the three measurement points. A smaller *Dev* value indicates more uniform cooling and implies that the simulation results more closely approximate the ideal conditions observed in actual production.

Table 3 compares the average cooling rates and their standard deviations at each measurement point obtained from the three simulations and the experiments. All numerical models predict lower absolute average cooling rates than the experimental measurements. This systematic underprediction may partly result from model simplifications, including the adiabatic-wall assumption and differences between idealized dry air and the actual compressed-air conditions. However, the individual contributions of these factors were not quantified in the present study. Despite the systematic underprediction of absolute cooling rate magnitude, the relative deviation of cooling uniformity Dev between simulation and experiment remains a valid index for quantitative comparison of two dynamic mesh methods. The data indicate that, in the stationary condition, the failure to account for the "temperature homogenization" effect caused by rail movement results in the largest differences in cooling rates among the three points, with the *Dev* value deviating from the experimental result by as much as 92.59 %. For the sliding mesh motion simulation, the *Dev* deviation from the experiment is 7.41 %, whereas the overset mesh motion simulation achieves a *Dev* deviation of only 22.22 %. These results indicate that both dynamic mesh techniques provide closer agreement with the experimental cooling-uniformity result than the stationary model.

 https://doi.org/10.64486/m.66.2.4

Table 3. Comparison of average cooling rates and standard deviations among three simulations and experiment

Simulation Type	A / ℃/s	B / ℃/s	C / ℃/s	$\overline{X}$ / ℃/s	*Dev* / ℃/s
Stationary State	6.98	6.25	7.26	6.83	0.52
Sliding Mesh Motion	7.26	6.75	6.76	6.92	0.29
Overset Mesh	8.46	7.85	7.92	8.08	0.33
Experimental value	8.85	9.39	9.12	9.12	0.27

Mechanism analysis for the performance difference between the two dynamic mesh methods. The overset mesh method allows the foreground mesh to move freely within the background mesh, and it transmits information across the overlapping regions using high-order interpolation algorithms. This approach enables more precise capture of the gradients in both the flow and temperature fields near moving boundaries which contributes to its higher accuracy in overall temperature field prediction. The different cooling-uniformity predictions of the two dynamic mesh methods may be related to their different data-transfer mechanisms. In the overset mesh method, interpolation across overlapping-grid boundaries may introduce small numerical fluctuations during reciprocating motion. In contrast, the direct flux transfer across the sliding interface may contribute to the closer agreement of the sliding-mesh model with the experimental cooling-uniformity result. However, these mechanisms were not separately quantified in the present study. Moreover, the overset mesh exhibits superior adaptability to complex irregular geometries, maintaining high-quality body-fitted meshes on the rail surface, thereby more accurately resolving the thermal boundary layer near the walls. For the current rectangular steel block with simple geometry and unidirectional translational motion, the fixed sliding interface may contribute to the closer agreement observed with the experimental cooling-uniformity result.

5. Discussion

This study compares the performance of the overset mesh and sliding mesh techniques in simulating air-jet cooling of a moving steel block; however, certain limitations remain. First, the mean relative temperature prediction error of the overset mesh model is 1.52 percentage points lower than that of the sliding mesh model. The overset mesh model produced consistently lower relative temperature errors than the sliding mesh model at the evaluated monitoring points and time instants. In terms of cooling-uniformity prediction, the sliding mesh model shows closer agreement with the experimental result, with a relative deviation of 7.41 %, compared with 22.22 % for the overset mesh model. It should also be noted that the sliding mesh model uses fewer mesh cells than the overset mesh model.

Second, the experiments measured only surface temperatures and did not capture the internal temperature distribution of the steel block or the microstructure after cooling. Future work could include internal temperature measurements and metallographic observations to further validate the numerical models.

Third, this study focused primarily on prediction accuracy and did not provide a detailed comparison of the computational efficiency of the two methods. Future investigations should include a more comprehensive performance assessment in terms of the number of mesh cells, computational time, memory requirements, time-step sensitivity, and convergence behaviour. Such analyses would provide a more complete basis for selecting the appropriate dynamic mesh method for in-line rail heat-treatment simulations.

6. Conclusions

1. This study applies both the overset mesh and sliding mesh techniques to the transient convective heat-transfer simulation of air-jet cooling of moving high-temperature steel blocks, providing a feasible approach for modelling coupled flow, solid motion and heat transfer during the heat treatment of moving workpieces.

2. By comparison with the experimental data, the numerical simulations that account for the movement of the steel block show better agreement in temperature-field prediction than the stationary simulation. The

https://doi.org/10.64486/m.66.2.4

sliding mesh and overset mesh techniques reduce the mean relative error from 18.01 % in the stationary case to 14.88 % and 13.36 %, respectively.

3. For cooling-uniformity prediction, evaluated using the sample standard deviation of the cooling rates at the three surface measurement points, the stationary simulation shows the largest relative deviation from the experimental result (92.59 %). The corresponding deviations are 7.41 % for the sliding mesh model and 22.22 % for the overset mesh model. Under the present working conditions, both dynamic mesh models show closer agreement with the experimental cooling-uniformity result than the stationary model, with the sliding mesh model showing the closest agreement.

4. Overall, the two dynamic mesh techniques show different advantages under the conditions investigated in this study. The overset mesh model provides the lowest mean relative temperature error, whereas the sliding mesh model shows closer agreement with the experimental cooling-uniformity result and uses fewer mesh cells. Further investigations of computational time, memory requirements, convergence behaviour and more complex workpiece geometries are needed before broader recommendations can be made regarding the selection of the two methods for industrial applications.

References

[1] J. Li, X. Zhao, H. Zhang, et al., "Numerical simulation of single-jet impact cooling and double-jet impact cooling of hot-rolled L-shaped steel based on multiphase flow model," Sci. Rep., vol. 14, Art. no. 4965, 2024, https://doi.org/10.1038/s41598-024-55567-8

[2] M. W. Hu, X. Hu, Q. B. Lv, et al., "Numerical simulation of air-jet cooling for rail joints with weld beading [in Chinese]," MW *Metal Forming*, vol. 11, pp. 50–59, 2024, https://link.cnki.net/urlid/11.5627.th.20240624.1513.002

[3] V. Anisiuba, H. Ma, A. Silaen, and C. Zhou, "Computational Studies of Air-Mist Spray Cooling in Continuous Casting," *Energies,* vol. 14, no. 21, Art. no. 7339, 2021, https://doi.org/10.3390/en14217339

[4] J. J. Fei, et al., "Research on the heat treatment process of U75V rail based on the coupling relationship between wheel railwear and rolling contact fatigue [in Chinese]," Ph.D. dissertation, Faculty of Materials Science and Engineering, Wuhan University of Science and Technology, Wuhan, China, 2023, https://doi.org/10.27380/d.cnki.gwkju.2023.000003

[5] J. H. Wu, "Numerical simulation of normalizing cooling process of U75V based on fluent [in Chinese]," MA thesis, School of Physical Sciences and Engineering, Beijing Jiaotong University, Beijing, China, 2021, https://doi.org/10.26944/d.cnki.gbfju.2021.001281

[6] L. P. Song, "Research on supersonic quench flow field and temperature field of U75V heavy rail [in Chinese]," MA thesis, School of Mechanical Engineering & Automation, University of Science and Technology Liaoning, Liaoning, China, 2021, https://doi.org/10.26923/d.cnki.gasgc.2021.000323

[7] D. D. Chen, "Study on the effect of air cooling quenching temperature on performance of U75V 100 meter rail [in Chinese]," MA thesis, School of Mechanical Engineering & Automation, University of Science and Technology Liaoning, Liaoning, China, 2022, https://doi.org/10.26923/d.cnki.gasgc.2022.000212

[8] L. P. Zhang, X. G. Deng, H. X. Zhang, et al., "Overview of advances in dynamic grid generation technology and unsteady computation methods [in Chinese]," *Advances in Mechanics*, vol. 40, no. 04, pp. 424–447, 2010, https://doi.org/10.6052/1000-0992-2010-4-J2009-123

[9] J. Dürrwächter, M. Kurz, P. Kopper, et al., "An efficient sliding mesh interface method for high-order discontinuous Galerkin schemes," *Computers & Fluids*, vol. 217, Art. no. 104825, 2021, https://doi.org/10.1016/j.compfluid.2020.104825

[10] P. Li, Z. X. Gao, C. W. Jiang, et al., "The progress of the overlapping grid techniques [in Chinese]," *Mechanics in Engineering*, vol. 36, no. 05, pp. 551–565, 2014, https://doi.org/10.6052/1000-0879-14-011

[11] A. J. Lang, D. P. Connolly, G. de Boer, S. Shahpar, B. Hinchliffe, and C. A. Gilkeson, "A review of Hyperloop aerodynamics," *Computers & Fluids*, vol. 273, Art. no. 106202, 2024, https://doi.org/10.1016/j.compfluid.2024.106202

[12] J. J. Xu, Y. Xiong, Z. Z. Wang, et al., "Numerical simulation of cavitation performance of HCRSP in steering conditions [in Chinese]," *Journal of Harbin Engineering University*, vol. 39, no. 12, pp. 1873–1879, 2018, https://doi.org/10.11990/jheu.201706021

[13] D. P. Zhang, J. Yan, B. W. Zhao, et al., "Numerical simulations of submarine rotating arms based on overset mesh [in Chinese]," *Science Technology and Engineering*, vol. 22, no. 1, pp. 393–399, 2022, https://doi.org/10.3969/j.issn.1671-1815.2022.01.048

[14] M. Chen, N. Zhang, J. J. Chen, et al., "Numerical research on free running model maneuvering motion of a generic submarine based on overset mesh [in Chinese]," *Journal of Ship Mechanics*, vol. 28, no. 04, pp. 485–500, 2024, https://doi.org/10.3969/j.issn.1007-7294.2024.04.002

[15] H. F. Zhou, "Research on hydrodynamic characteristics of position and attitude manipulation of underwater robot under the control of propeller, hydrofoil and center of gravity [in Chinese]," MA thesis, School of Civil Engineering & Transportation, South China University of Technology, Guangzhou, 2023, https://doi.org/10.27151/d.cnki.ghnlu.2023.003734

[16] F. Zhao, C. Qi, W. B. Li, et al., "Research on the relationship between pressure wave amplitude and vehicle speed during the non-constant-speed open-line intersection of high-speed trains [in Chinese]," *Railway Locomotive & Car*, vol. 41, no. 04, pp. 15–20, 2021, https://doi.org/10.3969/j.issn.1008-7842.2021.04.03

[17] C. Bojanowski, S. A. Lottes, and M. A. Sitek, CFD Estimation of Truck-Induced Wind Gusts on Variable Message Signs. Argonne, IL, USA: Argonne National Laboratory, 2019, https://doi.org/10.2172/1546789

[18] R. Koomullil, B. Soni, R. Singh, et al., "A Comprehensive Generalized Mesh System for CFD Applications," *Mathematics and Computers in Simulation*, vol. 78, no. 5–6, pp. 605–617, 2008, https://doi.org/10.1016/j.matcom.2008.04.005

[19] P. Wang, J. Lv, M. Bai, et al., "Numerical investigation of the flow and heat behaviours of an impinging jet," *International Journal of Computational Fluid Dynamics*, vol. 28, no. 6–10, pp. 301–315, 2014, https://doi.org/10.1080/10618562.2014.929119

[20] B. Yang, S. Chang, H. Wu, et al., "Experimental and numerical investigation of heat transfer in an array of impingement jets on a concave surface," *Applied Thermal Engineering*, vol. 127, pp. 473–483, 2017, https://doi.org/10.1016/j.applthermaleng.2017.07.190

 https://doi.org/10.64486/m.66.2.4